SiC-based power electronics building blocks for transformerless partial voltage converters

Thierry MEYNARD [1], Pier Paolo BEMBICH [2], Jérémy MARTIN [2]
[1] LAPLACE CNRS 2 rue Camichel, F31071 Toulouse, France
[2] Univ. Grenoble Alpes, CEA, Liten, Campus Ines, 73375 Le Bourget du Lac, France

***ABSTRACT* — Partial Power Converters (PPCs) are a promising solution in power conversion systems due to their potential for reduced cost, weight, volume, and power losses. This paper presents a Transformer-Less Partial Voltage Converter (TLPVC) designed to regulate the currents in multi-MPPT photovoltaic systems, avoiding the use of bulky and lossy transformers often required in conventional PPC architectures. The proposed topology enables semiconductors with a lower voltage rating, while also supporting grounding configurations to mitigate Potential Induced Degradation (PID) and ensuring fault tolerance. Comparative simulations between the TLPVC with a reference architecture have been carried out to evaluate its performance.**

Keywords—Partial Power Converter, Partial Voltage Converter, SiC power modules, PEBB, photovoltaics, High Power, high-efficiency power electronics.

1. INTRODUCTION

A strategy to enhance the performance of a power conversion system is to adopt a partial power processing approach. In such systems, the converter handles only a portion of the source power, while the remaining energy is transferred directly to the output. This configuration minimizes power losses and improves overall system efficiency, as most of the generated power bypasses additional conversion stages and reaches the load with virtually no loss [1].

The idea of the Partial Power Converter (PPC) was originally introduced in the aerospace sector, where reducing the weight and size of onboard equipment is essential. Due to its inherent advantages such as high efficiency, robustness, and compactness this solution has found application in a wide range of domains [2]. Numerous studies in the literature refer to PPC technology in various contexts, including on-board chargers for electric vehicles [3], energy storage system (ESS), fuel cell multi-stack systems [4], photovoltaics and other renewable energy sources.

This paper investigates a Transformer-Less Partial Voltage Converter (TLPVC). The core principle of the TLPVC is to switch only a fraction of the source voltage with the higher of the two voltages, rather than switching the higher voltage directly. This partial switching method allows the use of semiconductors with lower voltage ratings, reducing costs and enabling better trade-offs between switching speed and switching losses. Additionally, it permits the use of smaller filters (with lower inductance and capacitance) without compromising ripple control, which further reduces the system's volume, energy losses, and cost.

In the TLPVC, semiconductors can be selected with a lower voltage rating, along with other features such as modularity and current control in the multi-MPPT section. It also allows grounding configurations [5] to prevent the Potential Induced Degradation (PID) effect [6] and is fault-tolerant. This article will first explain the general concept of partial voltage conversion for PV systems. The TLPVC architecture will then be presented in the following sections. Finally, we will present simulations comparing the losses in a TLPVC converter alongside a comparison with the reference architecture.

2. THE PARTIAL VOLTAGE CONVERSION PRINCIPLE

The principle of partial voltage conversion can be seen in the circuit of Fig. 1, where only a fraction of the output voltage (V_{HV}) is applied to the two switches. The behavior of the circuit indicates the presence of an average current flow towards the capacitive midpoint and for this reason, the voltages across the capacities cannot be stabilized. However, this issue can be overcome, and the article presents a potential solution that may be of interest.

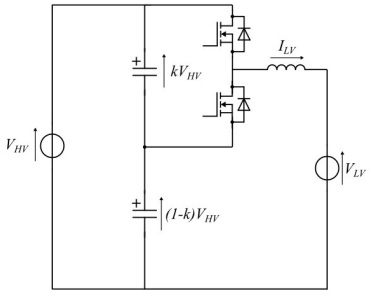

Fig. 1. Basic principle of Partial Voltage Conversion

2.1. Proposed Architectures for the MPPT [5]

Fig. 2 shows how the concept of partial voltage conversion can be applied to solar power conversion. In this configuration, each subfield is connected to a two-level boost converter (chopper) that regulates the subfield's voltage in order to achieve the maximum power point (MPP). This enables a modular and scalable structure, which will be discussed in more detail in the following sections and represents one of the main advantages of the proposed architecture. Since each subfield may be subject to different levels of irradiation, temperature, or ageing, there will be as many operating points as there are connected subfields. However, once the top and bottom rail voltages have stabilized, each converter can set its operating point and obtain the MPP for its corresponding subfield. Additionally, as can be seen in Fig. 2, only the difference between the v_{top} and v_{bot} voltages are

applied to the switches and this is advantageous as it allows the selection of semiconductors with a lower voltage rating. The next step is to explain how the two voltages v_{top} and v_{bot} can be stabilized. The solution found in the article will be presented in the following sections.

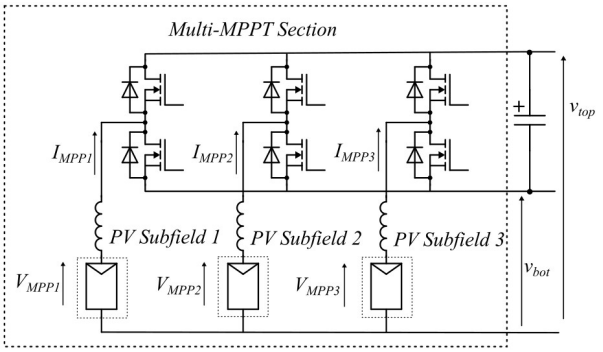

Fig. 2. Architecture for Multi-MPPT

3. Maximum Power Point Tracking of PV Subfields

In order to extract the maximum power (P_{MPP}) from a photovoltaic (PV) subfield, the voltage (V_{MPP}) imposed on the subfield must be adjusted. This operating voltage must be adapted according to variations in solar irradiance (G in W/m²) and temperature (T in °C), which the PV field is exposed to. As shown in Fig. 3, however, the voltage range within which the maximum power points occur is relatively narrow (between 830 V at T = 80 °C and 1.220 kV at T = −20 °C for a 1.5 kV PV field). This is advantageous for converter design, as it allows switches with a limited voltage rating to be used, thereby reducing costs and improving the device's overall performance.

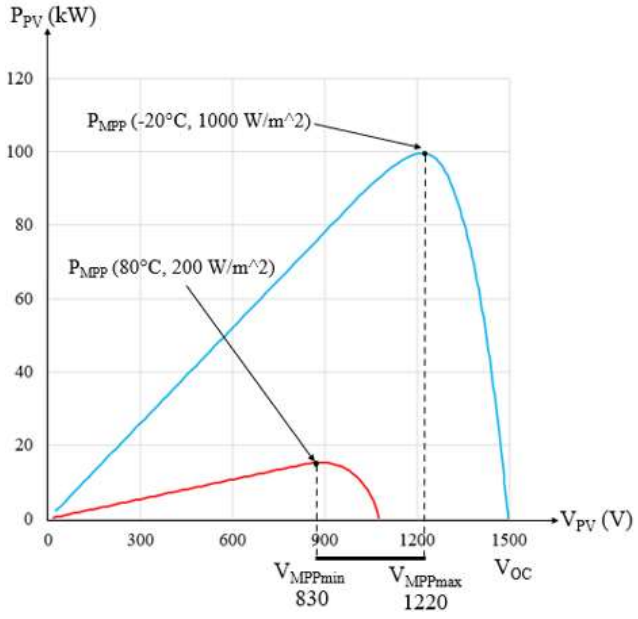

Fig. 3. Example of power-voltage characteristic of a PV subfield at different solar irradiances and two different temperatures; maximum power points and corresponding voltage interval is shown

4. Comparisons Of Topologies

4.1. *Flying Bus Twin Inverter Topology (FBTI) [5]*

One possible configuration for regulating the voltage of the top and bottom rails is shown Fig. 4. Three PV subfields are connected to three legs, and all the currents supplied by the PV field to the top and bottom rails of the floating bus, must be processed in order to transfer power to the rest of the system. The power product by the field is transferred to the AC grid via two Voltage Source Inverters (VSI top, VSI bot) in the proposed configuration.

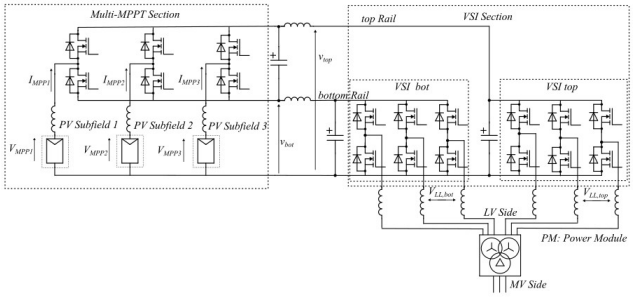

Fig. 4. Multi-MPPT in partial voltage operation connected to Twin Inverters: power is transferred to the grid via two VSI

The two VSI can adjust the top and bottom rails to the desired voltage, in accordance with the following equations:

$$\begin{cases} v_{bot} \leq V_{MPPmin} \\ V_{MPPmax} \leq v_{top} \end{cases} \quad (1)$$

The equation (1) show how v_{top} should be greater than the maximum subfield voltage, while v_{bot} should be less than the minimum subfield voltage. This ensures that all possible work points are covered and that each subfield can be adjusted to produce its MPP. The two voltages, v_{top} and v_{bot}, can be chosen arbitrarily, provided they satisfy equation (1). These voltages can be kept fixed, with v_{top} corresponding to the V_{MPP} of maximum radiation and minimum temperature, and v_{bot} corresponding to the V_{MPP} of minimum radiation and maximum temperature that the PV generator can be exposed to. In this paper, fixed voltages for v_{top} and v_{bot} have been chosen for the simulation section.

However, it is also possible to adjust the two voltages to achieve specific goals, such as balancing the currents in the top and bottom rails, or distributing the power equally between the two inverters. Having two inverters connected in parallel may increase the cost of the device; therefore, additional advantages must be provided to justify this increase in cost. Having two inverters in parallel in high-power photovoltaic plants could be beneficial if the operational rating of each inverter could be halved. In this case, the additional costs would be minimised.

The presented architecture also has good fault tolerance. In fact, it can continue to operate even if one of the output inverters fails, operating with the remaining VSI. While the remaining inverter cannot operate each subfield at its optimal voltage V_{MPP}, a suboptimal operating point can be achieved by exploiting the maximum power that the inverter can process.

4.2. *Reference Topology*

To evaluate the performance of the proposed converter, a reference architecture was implemented and simulated. In conventional architectures, each PV subfield is connected to a boost converter sized to handle the current generated by the subfield, as well as a voltage greater than the maximum voltage of the PV array, including a margin for reliability in accordance with common design practice. For higher power levels, multiple boost converters are connected in parallel and interfaced with a

VSI, which connects to the grid. Fig. 5 shows the reference architecture used for comparison.

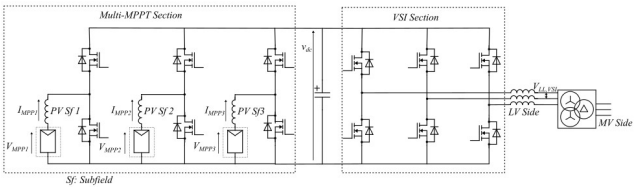

Fig. 5. Reference Architecture

4.3. Topologies sizing and power modules selection

This section outlines the configuration used for the simulations in both systems. These simulations were carried out using the PLECS software.

Each PV subfield consists of a number of panels connected in series and in parallel to achieve a V_{OC} of 1500V and a maximum power output of ~250 kW. Three subfields are used in the simulations. Each subfield is connected in parallel to the VSI section via a boost converter, which provides the maximum power point tracking (MPPT). The total maximum power injected into the line is therefore 750 kW. Connection to the three-phase MV line can be made via a transformer, which enables the AC voltage level of the inverter to be selected. The Table 1 shows the voltages used in the simulation.

Table 1. Output Voltages and line RMS currents of VSIs

Reference Architecture	Flying Bus Twin Inverter (FTBI)	
$V_{LL,\ VSI}$ = 850V 3~ 50Hz	$V_{LL,\ VSI\ bot}$ = 500V 3~ 50Hz	$V_{LL,\ VSI\ top}$ = 850V 3~ 50Hz
$I_{L,\ RMS}$ = 524A	$I_{L,\ RMS}$ = 227A	$I_{L,\ RMS}$ = 389A

To calculate the losses and efficiency, the module case temperature is set at 75 °C, with a junction temperature that must not exceed 150 °C for any case studied.

All power modules are made up of silicon carbide (SiC) metal-oxide-semiconductor field-effect transistors (MOSFET). Table 2 reports, voltage and current ratings of each power module.

Table 2. Power modules selection (SiC MOSFET based)

Reference Architecture	Flying Bus Twin Inverter (FBTI)		
MULTI-MPPT & VSI	Multi-MPPT	VSI bot	VSI top
2300V / 5mΩ	900V / 2.5 mΩ	1200V / 2.67 mΩ	2300V / 5mΩ

Once the power modules for the simulation had been selected, the PLECS model was implemented to allow the number of power modules connected in series (n_s) or in parallel (n_p) to be scaled.

4.3.1. Reference architecture

The total number of power modules for the Multi-MPPT and VSI building blocks in the reference architecture is:

- (n_p = 1) × 3 legs = 3
- (n_p = 2) × 3 legs = 6

for a total of nine power modules.

4.3.2. Flying bus twin inverter

The Multi-MPPT section and the bottom VSI do not require modules in parallel (n_p = 1), whereas the top VSI does (n_p = 2). The Flying Bus Twin Inverter consists of a total of 12 power modules. Table 3 shows the number of power modules required for each architecture.

Table 3. Total number power modules for each architecture

Architecture	Multi-MPPT section		Inverter			Total
Reference (750kW)	n_s = 1 n_p = 1	3		n_s = 1 n_p = 2	6	2.3kV: 9
FBTI (750kW)	n_s = 1 n_p = 1	3	bot	n_s = 1 n_p = 1	3	900V: 3 1.2kV: 3 2.3kV: 6
			top	n_s = 1 n_p = 2	6	

As previously mentioned, the simulations were conducted by keeping the voltages v_{top} and v_{bot} constant. These were set to 1400 V and 830 V, respectively. The DC link voltage of the reference architecture is equal to v_{dc} = 1400 V. The switching frequency of the semiconductors was set to 10 kHz.

Different subfields were simulated by applying irradiance values ranging from 150 W/m² to 350 W/m². After a settling period, the irradiance was increased to 1000 W/m² for each subfield. Only irradiance was considered as an environmental variable, since variations in ambient temperature were not factored into the simulations.

5. SIMULATIONS RESULTS

This section presents the results obtained from the simulations. It was found that, for each operating point analyzed, the corresponding subfield was successfully brought to the MPP point by each boost converter, with current and voltage values in line with expectations.

In both cases, the output currents are sinusoidal and correctly phase-shifted with respect to each other. In the case of the Flying Bus Twin Inverter, the current amplitudes are higher in the top VSI than in the bottom VSI, indicating that, with the selected values of v_{top} and v_{bot}, the power sharing in the two VSIs are not equal by default.

5.1. Loss comparison

5.1.1. Multi-MPPT section

Table 4 shows the conduction and switching loss results for power modules.

Table 4. Losses Analysis Multi-MPPT Section (p.m. = power module)

Multi-MPPT Section				
P_{MPP} = 750kW, $Temp_{PV}$ = 25°C, V_{MPP} = 1200V, G = 1000W/m², F_{SW} = 10kHz				
	REFERENCE 1 p.m. of 2.3kV / Leg 1Leg = 1 chopper		FBTI 1 p.m. of 900V / Leg 1Leg =1chopper	
	bot MOS	top MOS	bot MOS	top MOS
Junction Temperature	92°C	113°C	100°C	87°C
Conduction Losses per module	419W		146W	
Conduction losses for the 3 choppers	1257W		438W	
Switching Losses per module	107W		136W	
Switching losses for the 3 choppers	321W		408W	
Total Losses	1578W		846W	

The modules used in the 2.3kV-rated reference architecture are more resistive than those used in the 900V-rated FBTI architecture. Conduction losses are approximately three times higher in the reference architecture than in the FBTI architecture. Switching losses, on the other hand, are fairly similar, probably because the 900 V module chips are larger and more capacitive, which negatively affects performance compared to the reference architecture. Overall, the multi-MPPT section incurs losses that are almost half as much for the partial power architecture (FBTI) as for the reference architecture.

5.1.2. VSI Section

Table 5 shows the results for the voltage inverter section obtained for the reference case and for the case using partial voltage conversion (FBTI). Conduction losses are approximately halved for the FBTI architecture compared to the reference architecture. Switching losses are slightly lower for the reference architecture. In any case also in this section, the FBTI topology exhibits lower total losses than the reference architecture.

Table 5. Loss Analysis VSI Section (p.m. = power module)

VSI Section			
P_{MPP} = 750kW, Temp $_{PV}$ = 25°C, V_{MPP} = 1200V, G = 1000W/m², F_{SW} = 10kHz			
	REFERENCE 2 p.m. of 2.3kV / Leg	FBTI	
		VSI bot 1 p.m. of 1.2kV /Leg	VSI top 2p.m./Leg of 2.3kV /Leg
Junction Temperature	120°C	87°C	97°C
Conduction Losses per module	745W	154W	325W
Conduction Losses VSIs	4470W	462W	1950W
Switching Losses per module	135W	166W	93W
Switching Losses VSIs	810W	498W	558W
Total Losses	5280W	3468W	

5.1.3. Recap of loss

Analysis of the two systems shows that the partial power converter is more efficient, with approximately 40% less loss. This is due to the ability to implement chips with superior conduction performance and current ratings (size) in the 900V rated power modules than in the 2.3 kV power modules. The junction temperatures shown in the comparison tables suggest that both conversion systems have an important power margin.

6. CONCLUSIONS

This article presents an innovative conversion structure for photovoltaic (PV) plants. The converter can impose a lower voltage on the switches, enabling the use of power modules with lower voltage rating. The proposed architecture offers additional advantages, such as modularity. This allows multiple subfields to be connected to individual MPPT choppers, on which the voltage rating is reduced.

In addition, this structure allows for multiple grounding configurations [5]. This makes it possible, with the necessary knowledge, to eliminate polarity signs that activate PID effects. It also has good fault tolerance; in the event of a malfunction in one of the VSI units connected to the grid, the device can continue to operate by driving the subfields to a sub-optimal operating point. The article presents simulation results evaluating the performance of the proposed converter. These showed that the device could control the voltage across the different subfields at every operating point, achieving maximum power points (MPPs) and providing consistent voltage and current values. During the simulation phase, the Flying Bus Twin Inverter was also compared with a standard photovoltaic (PV) architecture, referred to in the article as the 'Reference Architecture'. It was found that the losses of the Flying Bus Twin Inverter were reduced by almost a factor of 2 compared to the Reference Architecture.

These studies have demonstrated a promising new PV plant conversion architecture. In future, construction of a full-power prototype, laboratory testing and testing in a real PV field will be necessary to validate the simulations reported in this article. Furthermore, operating with higher-voltage PV strings (3 kV) using this architecture appears promising, and further studies will be carried out to explore this possibility [7].

THIS PUBLICATION INCORPORATES INNOVATIVE TECHNOLOGIES THAT ARE CURRENTLY PATENT PENDING [5]

7. REFERENCES

[1] J. R. Rakoski Zientarski, J. R. Pinheiro, M. L. da Silva Martins, and H. L. Hey, 'Understanding the partial power processing concept: A case-study of buck-boost dc/dc series regulator', in *2015 IEEE 13th Brazilian Power Electronics Conference and 1st Southern Power Electronics Conference (COBEP/SPEC)*, Nov. 2015, pp. 1–6. doi: 10.1109/COBEP.2015.7420092.

[2] O. Abdel-Rahim, A. Chub, A. Blinov, and D. Vinnikov, 'Series Buck-Boost Partial Power Converter based on the Push-Pull converter', in *IECON 2022 – 48th Annual Conference of the IEEE Industrial Electronics Society*, Oct. 2022, pp. 1–5. doi: 10.1109/IECON49645.2022.9968574.

[3] M. Wu, I.-W. Iam, and C.-S. Lam, 'High-Efficiency Wireless Integrated On-Board Charger System Using Partial Power Conversion', *IEEE Trans. Power Electron.*, pp. 1–13, 2025, doi: 10.1109/TPEL.2025.3528130.

[4] I. Siad, A. Battiston, T. Leroy, J.-P. Martin, and S. Pierfederici, 'Exploration of Partial Power Converter Topology for Fuel Cell Multi-Stack Systems in Heavy-Duty Applications', in *2024 IEEE International Conference on Electrical Systems for Aircraft, Railway, Ship Propulsion and Road Vehicles & International Transportation Electrification Conference (ESARS-ITEC)*, Nov. 2024, pp. 1–7. doi: 10.1109/ESARS-ITEC60450.2024.10819856.

[5] T. Meynard, J. Martin, and P. P. Bembich, 'Dispositif de conversion d'énergie'

[6] W. Zhang, Y. Wang, P. Xu, D. Li, and B. Liu, 'A potential induced degradation suppression method for photovoltaic systems', *Energy Rep.*, vol. 10, pp. 3955–3969, Nov. 2023, doi: 10.1016/j.egyr.2023.10.064.

[7] A. Bier, O. Wiss, and P. Messaoudi, 'A 3 kV, 18 kW medium-voltage PV plant demonstrator', 2017.